

# The Mpemba effect in spin glasses is a persistent memory effect

Marco Baity-Jesi<sup>a,b</sup>, Enrico Calore<sup>c</sup>, Andres Cruz<sup>d,b</sup>, Luis Antonio Fernandez<sup>e,b</sup>, José Miguel Gil-Narvión<sup>b</sup>, Antonio Gordillo-Guerrero<sup>f,g,b</sup>, David Iñiguez<sup>b,h</sup>, Antonio Lasanta<sup>i</sup>, Andrea Maiorano<sup>j,b</sup>, Enzo Marinari<sup>k</sup>, Victor Martin-Mayor<sup>e,b</sup>, Javier Moreno-Gordo<sup>b,d</sup>, Antonio Muñoz Sudupe<sup>e,b</sup>, Denis Navarro<sup>l</sup>, Giorgio Parisi<sup>k,1</sup>, Sergio Perez-Gavero<sup>m,b,d</sup>, Federico Ricci-Tersenghi<sup>k</sup>, Juan Jesus Ruiz-Lorenzo<sup>n,g,b</sup>, Sebastiano Fabio Schifano<sup>o</sup>, Beatriz Seoane<sup>p,q,b</sup>, Alfonso Tarancón<sup>d,b</sup>, Raffaele Tripiccione<sup>c</sup>, and David Yllanes<sup>r,b,s,1</sup>

<sup>a</sup>Department of Chemistry, Columbia University, New York, NY 10027, USA; <sup>b</sup>Instituto de Biocomputación y Física de Sistemas Complejos (BIFI), 50018 Zaragoza, Spain; <sup>c</sup>Dipartimento di Fisica e Scienze della Terra, Università di Ferrara e INFN, Sezione di Ferrara, I-44122 Ferrara, Italy; <sup>d</sup>Departamento de Física Teórica, Universidad de Zaragoza, 50009 Zaragoza, Spain; <sup>e</sup>Departamento de Física Teórica, Universidad Complutense, 28040 Madrid, Spain; <sup>f</sup>Departamento de Ingeniería Eléctrica, Electrónica y Automática, U. de Extremadura, 10003, Cáceres, Spain; <sup>g</sup>Instituto de Computación Científica Avanzada (ICCAEx), Universidad de Extremadura, 06006 Badajoz, Spain; <sup>h</sup>Fundación ARAID, Diputación General de Aragón, Zaragoza, Spain; <sup>i</sup>Gregorio Millán Institute of Fluid Dynamics, Nanoscience and Industrial Mathematics, Department of Materials Science and Engineering and Chemical Engineering, Universidad Carlos III de Madrid, 28911 Leganés, Spain; <sup>j</sup>Dipartimento di Fisica, Sapienza Università di Roma, I-00185 Rome, Italy; <sup>k</sup>Dipartimento di Fisica, Sapienza Università di Roma, INFN, Sezione di Roma 1, and CNR-Nanotec, I-00185 Rome, Italy; <sup>l</sup>Departamento de Ingeniería, Electrónica y Comunicaciones and I3A, U. de Zaragoza, 50018 Zaragoza, Spain; <sup>m</sup>Centro Universitario de la Defensa, Carretera de Huesca s/n, 50090 Zaragoza, Spain; <sup>n</sup>Departamento de Física, Universidad de Extremadura, 06006 Badajoz, Spain; <sup>o</sup>Dipartimento di Matematica e Informatica, Università di Ferrara e INFN, Sezione di Ferrara, I-44122 Ferrara, Italy; <sup>p</sup>Sorbonne Universités, CNRS, IBPS, Laboratoire de Biologie Computationnelle et Quantitative - UMR 7238, 4 place Jussieu, 75005 Paris, France; <sup>q</sup>Sorbonne Universités, Institut des Sciences du Calcul et des Données, 4 place Jussieu, 75005 Paris, France; <sup>r</sup>Department of Physics and Soft and Living Matter Program, Syracuse University, Syracuse, NY, 13244; <sup>s</sup>Chan Zuckerberg Biohub, San Francisco, CA 94158

This manuscript was compiled on July 9, 2019

**The Mpemba effect occurs when a hot system cools faster than an initially colder one, when both are refrigerated in the same thermal reservoir. Using the custom built supercomputer Janus II, we study the Mpemba effect in spin glasses and show that it is a non-equilibrium process, governed by the coherence length  $\xi$  of the system. The effect occurs when the bath temperature lies in the glassy phase, but it is not necessary for the thermal protocol to cross the critical temperature. In fact, the Mpemba effect follows from a strong relationship between the internal energy and  $\xi$  that turns out to be a sure-tell sign of being in the glassy phase. Thus, the Mpemba effect presents itself as an intriguing new avenue for the experimental study of the coherence length in supercooled liquids and other glass formers.**

Spin glasses | memory effects | Mpemba effect | non-equilibrium physics

The Mpemba effect (ME) refers to the observation that the hotter of two identical beakers of water, put in contact with the same thermal reservoir, can cool faster under certain conditions (1). The phenomenon is not specific to water, as it has been reported for nanotube resonators (2) and clathrate hydrates (3). However, although records of the ME date as far back as Aristotle (4, 5), its very existence has been questioned (6).

The ME is a non-equilibrium process (7–9) and when a complex system evolves out of equilibrium its past history determines its fate. The simplest of these memory effects is, probably, the Kovacs effect (10): after a temperature cycle, a glassy polymer is left at the working temperature  $T$  with a specific volume equal to its equilibrium value. Yet, the polymer is still out of equilibrium, as evinced by a non-monotonic further time evolution of the specific volume. Memory effects are ubiquitous and relevant in many systems of technological and/or biological interest. Important examples include disordered materials (11), polymers (12), amorphous solids (13), granular matter (14), biological systems (15), batteries (16) and, of course, the disordered magnetic alloys known as spin glasses, which display spectacular memory effects (17).

Here, we show that spin glasses (18) are an especially apt model system to investigate the ME. Using the Janus II

supercomputer (19), custom built for spin-glass simulations, we show that the ME is indeed present in spin glasses and we clarify its origin: it is a non-equilibrium memory effect, encoded in the glassy coherence length.

One major advantage of spin glasses as a model system is that, while their behavior is very complex, we now know that many of their major non-equilibrium processes are ruled by the coherence length  $\xi$  of the growing glassy domains (20–23). This includes, as we show in this paper, the ME. In the simplest protocol, a sample initially at a high temperature is suddenly placed at the working temperature  $T$ , lower than the critical temperature  $T_c$ . The system relaxes afterwards, but

## Significance Statement

The Mpemba effect, wherein an initially hotter system relaxes faster when quenched to lower temperatures than an initially cooler system, has attracted much attention. Paradoxically its very existence is a hot topic. Using massive numerical simulations, we show unambiguously that the Mpemba effect is present in the archetypical model system for complex behavior, spin glasses. We find that the Mpemba effect in spin glasses is due to the aging dynamics of the internal energy, as controlled by the non-equilibrium spin-glass coherence length. Interestingly, the effect is not present when the system remains all the time in the paramagnetic phase. Therefore, the Mpemba effect suggest itself as an effective probe for a glass transition, potentially useful for other glass-forming systems.

A.L. and E.M. suggested undertaking this project; L.A.F., A.L., V.M.-M. and J.J.R.-L. designed the numerical experiment; the data analysis was performed by L.A.-F., A.L., V.M.-M., J.M.-G. and J.J.R.-L.; the physical interpretation of results contained in the manuscript was provided by A.L. and V.M.-M., with contributions from L.A.F., A.M., E.M., J.M.-G., G.P., F.R.-T., J.J.R.-L. and D.Y.; D.I., S.F.S., A.T., and R.T. contributed Janus II design; J.M.G.-N. and D.N. contributed Janus II simulation software; M.B.-J., E.C., A.C., L.A.F., J.M.G.-N., A.G.-G., D.I., A.M., J.M.-G., A.M.S., S.P.-G., S.F.S., A.T., and R.T. contributed Janus II hardware and software development; figures were contributed by M.B.-J., J.M.G., L.A.F. and B.S.; the paper was written by M.B.-J., A.L., V.M.-M., J.M.-G., J.J.R.-L., F.R.-T., B.S. and D.Y.

G.P. received funding from the Simons collaboration, and Srikanth Sastry has received travel expenses to attend the Simons collaboration annual meetings

<sup>1</sup> To whom correspondence should be addressed. E-mail: giorgio.parsi@roma1.infn.it, david.yllanes@cziobiohub.org

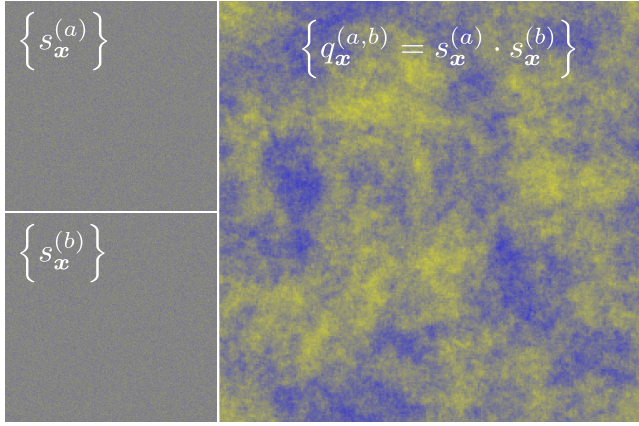


**Fig. 1. Spin-glass coherence length.** **Top left:** A snapshot of a configuration  $\{s_x^{(a)}\}$ , which has evolved for  $t = 2^{36}$  Monte Carlo steps at  $T = 0.7 \approx 0.64T_c$ . We show the average magnetization on the  $xy$  plane, averaging over  $z$ . **Bottom left:** Another configuration  $\{s_x^{(b)}\}$  of the same sample, prepared in the same way as  $\{s_x^{(a)}\}$ . No visible ordering is present in either configuration because the preferred pattern of the magnetic domains cannot be seen by eye ( $s = 1$  is plotted in yellow, and  $-1$  in blue). **Right:** If one measures the overlap between the two configurations, see Eq. (5) in Materials and Methods, and with the same color code used for the spins, the preferred pattern of the magnetic domains, of size  $\xi$ , becomes visible. A reliable method to extract  $\xi$  from the overlap fields has been known for some time (24), but only in 2018 has it been possible to reach accuracies better than 1% in  $\xi$  (25), thanks to the Janus II computer (19) and the use of many clones for the same sample (this strategy works only if the system size, which here is  $L = 160$ , turns out to be much larger than  $\xi$ ).

response functions such as the magnetic susceptibility depend on time for as long as one has the patience to wait (in analogy with living beings, glasses are said to age (12)). As aging proceeds, the size of the magnetic domains,  $\xi(t)$ , perennially grows (yet, the magnetic ordering is apparently random, see Fig.1).

Only recently have we learned how to compute  $\xi(t)$  reliably from microscopic correlation functions (24). Interestingly enough, this *microscopic*  $\xi(t)$  matches (23) the length scale determined from *macroscopic* responses in experiments (26).

The time growth of  $\xi(t)$  will be a crucial issue. In the paramagnetic phase,  $T > T_c = 1.102(3)$  (27),  $\xi$  grows up to its equilibrium value, which can be very large close to  $T_c$ . On the other hand, below  $T_c$ ,  $\xi(t)$  grows without bounds, but excruciatingly slowly. Empirically, one finds that  $t$  and  $\xi(t)$  are related through (25, 28)

$$\xi \propto t^{1/z(T)}, \quad z(T < T_c) \approx 9.6 \frac{T_c}{T}. \quad [1]$$

The exponent  $z(T)$ , already very large near  $T_c$ , becomes even larger upon lowering  $T$ . The very large value of  $z(T)$  explains why supercomputers such as Janus II, specifically designed to simulate spin glasses (19), are necessary. Indeed, one has to simulate the dynamics for a long time in order to see  $\xi(t)$  vary by a significant amount. The simulations discussed herein (see Ref. (25) and Materials and Methods) have  $t$  varying by 11 orders of magnitude, for systems large enough to be representative of the thermodynamic limit. On the other hand, for  $T > T_c$  Eq. (1) holds only out-of-equilibrium, when  $\xi$  has not yet approached its final equilibrium value. Under such circumstances,  $z \approx 6$  has been computed numerically (29).

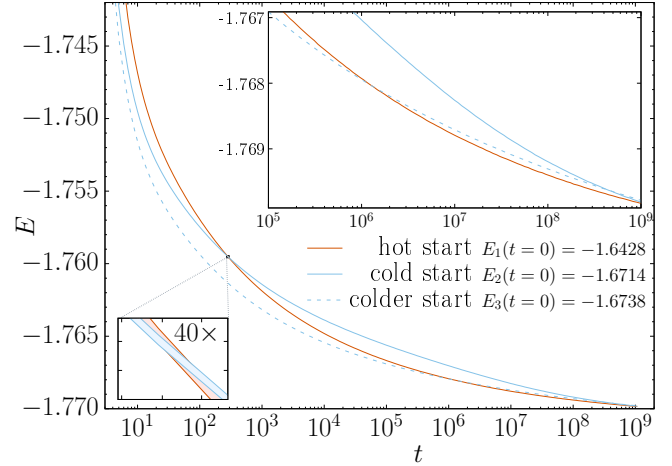


**Fig. 2. Classical Mpemba protocol.** We show the time evolution of the energy of spin glass systems initially prepared at a higher temperature ( $T = 1.3$ , red line) or at a lower temperature ( $T = 1.2$ , blue lines), but always in the paramagnetic (high-temperature) phase ( $T_c \approx 1.10$ ). In all three cases the systems are initially left to evolve out of equilibrium until they reach the internal energies shown in the figure key. At  $t = 0$  all preparations are quenched, that is, put in contact with a thermal reservoir at temperature  $T = 0.7 \approx 0.64T_c$ . As discussed in the text, the instantaneous internal energy is a measure of the (off-equilibrium) sample temperature. In agreement with the original Mpemba experiment (1), the system originally at the higher energy cools faster. **Bottom left inset:** Closeup of the first crossing between energy curves, showing the very small error bars, equal to the thickness of the lines (here and in all other figures, error bars represent one standard deviation; control variates, see (30) and Materials and Methods, are used to improve accuracy). **Top right inset:** Closeup of the second crossing between energy curves.

## Results

**The Mpemba effect in spin glasses.** The first step in a numerical study of the ME is identifying which thermometric magnitude corresponds to the off-equilibrium temperature that would be found experimentally. In our case, this is the energy density (i.e., the instantaneous energy per spin  $E$ , see Materials and Methods).  $E$  is a natural choice, because it is the observable conjugated with temperature. Furthermore, *in equilibrium*, there is a monotonically increasing correspondence between  $T$  and  $E$ .

After the above considerations, we are ready to investigate the ME in spin glasses (see Materials and Methods for details on the model and observables). Our first protocol strongly resembles the original Mpemba experiment (1). We study the evolution of two different non-equilibrium preparations for the same system: in preparation 1 the system starts in a thermal bath at  $T_1 = 1.3$  and is left to evolve until it reaches an initial energy  $E_1(t=0) \approx -1.6428$ , while in preparation 2 it is put in a bath at  $T_2 = 1.2$  where it reaches a much lower initial energy  $E_2(t=0) \approx -1.6714$ .\* Note that these states are out of equilibrium:  $T_1$  and  $T_2$  only indicate the temperature of the bath. At time  $t = 0$ , both systems are quenched, that is, they are placed in contact with a thermal reservoir at  $T = 0.7 \approx 0.64T_c$ . Fig. 2 shows the evolution of the energies (temperatures) after the quench: the hotter preparation (red) relaxes to low energies faster than the colder preparation (solid blue). This is a perfect correspondence with the ME (1).

We also show with a blue dotted line the evolution of a third

\*The configuration of the system before being exposed to either bath is random with a flat distribution (which is a typical  $T = \infty$  configuration).

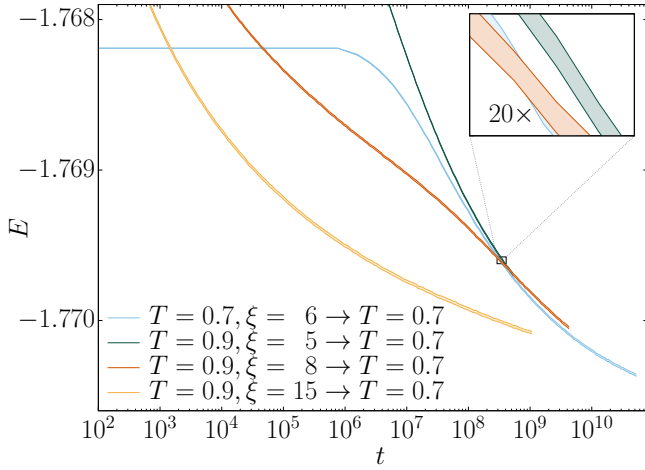


**Fig. 3. Mpemba effect in the spin-glass phase.** As in Fig. 2, but all four initial preparations (see text for details) are now carried out in the spin-glass phase ( $T < T_c$ ). The preparation that cools faster is not the initially coldest one (blue curve), but the one with the largest initial coherence length (yellow curve). The last point in the isothermal relaxation at  $T = 0.7$  corresponds with the same time as the configurations shown in Fig. 1. **Inset:** A zoom of the *second* crossing point between the curves for preparations ( $T = 0.9, \xi = 8$ ; red curve) and ( $T = 0.7, \xi = 6$ ; blue curve). This second crossing is not the ME. Rather, the ME arises at the *first* crossing at  $t \approx 5 \times 10^4$ . The second crossing disappears if one plots parametrically  $E(t)$  as a function of  $\xi(t)$ . In other words, the description afforded by Eq. (2) is very accurate, but not exact.

preparation, starting again at the lower temperature  $T = 1.2$ , but with a slightly lower initial energy  $E_3(t=0) \approx -1.6738$ . Even in this case the ME is present, but the crossing of the energy curves takes place at a much longer time, even though the difference between the preparation energies  $E_2$  and  $E_3$  is of only 0.15%. We need to find the controlling parameter.

Remembering our initial discussion of spin-glass dynamics a natural candidate emerges: the coherence length  $\xi(t)$ . Indeed, in terms of  $\xi$  our three starting conditions look very different. Our hot preparation ( $T_1 = 1.3, E_1 = -1.6428$ ) had  $\xi_1 = 12$ , while our cold preparations ( $T_{2,3} = 1.2, E_2 = -1.6714, E_3 = -1.6738$ ) had  $\xi_2 = 5$  and  $\xi_3 = 8$ , respectively. Therefore, upon quenching, the initially hotter preparation is actually in a more advanced dynamical state. In addition, preparations 2 and 3, which have almost the same  $E$ , have very different starting  $\xi$ , which, from Eq. (1), can explain the differing relaxation times.

We arrive, then, at our working hypothesis: out of equilibrium, our system is not adequately labeled by the temperature  $T$  of the thermal bath alone, or even by  $T$  plus the instantaneous internal energy  $E$ . Instead,  $\xi$  emerges as the hidden parameter that will rationalize the results.

Notice that, according to this idea, crossing  $T_c$  should not be necessary in order to find an ME. The only required ingredient would be starting points A and B with  $T_A > T_B$  and  $\xi_A > \xi_B$ . We test this hypothesis in Figure 3, where we work solely in the low-temperature phase. Preparation 1 starts at  $T = 0.7$  until it reaches  $\xi_1 = 6$ , while preparations 2–4 evolve at  $T = 0.9$  until they reach  $\xi = 5, 8, 15$ , respectively. All samples are then quenched to  $T = 0.7$  and we start measuring (i.e., we set  $t = 0$ ). In accordance with our previous discussion, the cooling rate is not controlled by the preparation temperature, but by the starting coherence length. Preparations starting at  $T = 0.9$  but with  $\xi(t=0)$  greater than  $\xi_1 = 6$  cool faster than preparation 1.

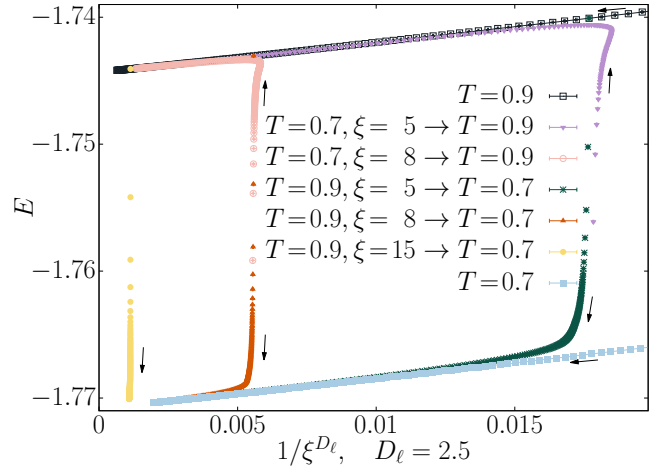


**Fig. 4. Relationship between the energy density  $E$  and the coherence length  $\xi$ .** As suggested by Eq. (2), for isothermal relaxations (in the plot  $T = 0.7$  and  $0.9$ , depicted with continuous lines)  $E$  is an essentially linear function of  $1/\xi^{2.5}$  (at least for the plotted range of  $\xi > 4.8$ ). Furthermore, the dependence of the slope on temperature is marginal. Temperature-varying protocols are seen to be essentially vertical moves between the straight lines corresponding to isothermal relaxations at the initial and final temperatures. These vertical moves are very quick initial transients, in which (in moves to higher temperatures only),  $\xi$  slightly decreases and then increases again.

**The energy-coherence length phase diagram.** In order to make these observations more quantitative, we need to explore the relationship between  $E$  and  $\xi$  in an off-equilibrium spin glass. Fortunately, we have heuristic arguments (31) and numerical results (20, 24) suggesting that

$$E(t) = E_\infty(T) + \frac{E_1}{\xi^{D_\ell}(t)} + \dots \quad [2]$$

The dots stand for scaling corrections, subdominant for large  $\xi$ , and  $D_\ell \approx 2.5$  (32) is the lower critical dimension (the phase transition occurs only for spatial dimension  $D > D_\ell$ ). We note that the heuristic derivation of Eq. (2), recall Ref. (31), makes sense only in the spin-glass phase,  $T < T_c$ . We shall test below and in our study of the inverse Mpemba Effect whether or not Eq. (2) applies in the spin-glass phase and in the paramagnetic phase.

As Fig. 4 shows, the ME in spin glasses follows from the combination of two simple ideas:

1. When a quick temperature change takes place,  $\xi$  [which is a slow variable, recall Eq. (1)] has no time to adjust and remains basically unchanged.
2. Setting quick transients aside, the energy density follows in all cases Eq. (2).

Both of these points are slight oversimplifications (the analysis of the deviations will be performed elsewhere) but their combination results in a very simple explanation of the ME. We first note that, when temperature is fixed, the energy density is an (almost) linear function of  $1/\xi^{2.5}$ . Furthermore, the slope  $E_1$  varies by less than 4% in the range we explore. It follows that the natural phase diagram to discuss the ME is the  $(E, 1/\xi^{2.5})$  plane. Indeed, isothermal relaxations are represented in the  $(E, 1/\xi^{2.5})$  plane as a set of (almost) parallel, (almost) straight lines. To an excellent first approximation, the effects of temperature changes can be depicted as almost instantaneous vertical

moves between the parallel straight lines that correspond to the initial and final temperatures. It then follows that, in the spin-glass phase at least, the larger the starting  $\xi$ , the faster the cooling, irrespective of the initial preparation protocol, exactly as observed in Figs. 2 and 3.

**Inverse Mpemba Effect.** In Refs. (7, 8) an inverse thermal protocol was suggested: the bath temperature was chosen to be higher than the one of the starting condition. Under such circumstances, it was observed that the coolest of two initial preparations could heat faster. This effect was named *inverse* ME (IME).

As we have seen in the discussion of the energy-coherence length phase diagram, heating and cooling protocols are quite symmetrical *provided that both the final and initial bath temperatures lie below  $T_c$* . It is therefore more challenging to see whether or not the IME survives crossing  $T_c$ . The question is non-trivial, because Eq. (2) does not hold in the paramagnetic phase.

To verify this, we reverse our protocol, choosing starting temperatures  $T < T_c$  in the spin-glass phase, and warm up the samples to a temperature well above  $T_c$ . Specifically, we use three starting conditions for the warm-up experiment. In protocol 1, we choose  $T = 0.7$  and  $\xi = 2.5$ ; in protocol 2, we choose  $T = 0.7$  and  $\xi = 11.7$ ; in protocol 3, we choose  $T = 0.8$  and  $\xi = 15.8$ . In the three cases, we switch instantly the thermal bath to  $T = 1.4$  [where the asymptotic equilibrium value is  $\xi = 8.95(5)$ ], and follow the relaxation of coherence length and energy.

Fig. 5 depicts the evolution of the energy in the warm-up experiments. If one compares protocol 1 with protocol 3, the ME is clearly absent. Instead, a tiny ME is present when comparing protocols 2 and 3, which have a more similar starting energy, and a coherence length that manifests a better thermalization in the spin glass phase: the curve that is initially hotter becomes colder after  $\sim 20$  iterations.

In Fig. 6, we show the evolution of  $\xi$  during the three warm-up protocols. Visibly, Eq. (1), valid only under  $T_c$ , does not hold. Furthermore, for all of the starting conditions the curves tend to approach a master curve represented by the instant quench from  $T = \infty$  to  $T = 1.4$ , generating an undershoot in the time evolution of the observable. An analogous independence of the initial conditions has been recently observed in the paramagnetic phase of a two-dimensional spin glass (33, 34).

By comparing Figs. 5 and 6, one can see that energy and coherence length converge to their equilibrium value at very different times, and that an undershoot on  $E(t)$  is not corresponded with an undershoot of  $\xi(t)$  (and vice versa). This decoupling between the two observables is necessary for the ME to take place, since the time scale of the crossing between protocols 2 and 3 does not correspond to any significative change in coherence lengths. The non-monotonic behavior of  $E(t)$  and  $\xi(t)$  will be the subject of further investigation.

## Discussion

In summary, we have shown that the Mpemba effect (ME) is present in spin glasses, where it appears as an intrinsically non-equilibrium process, ruled by the spin-glass coherence length  $\xi$ . Although encoding the history of a complex system by a single number is an oversimplification, we have shown that

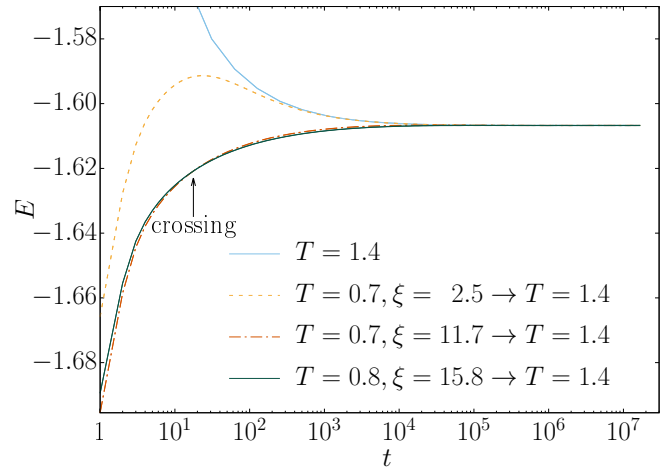


**Fig. 5. A tiny inverse Mpemba effect.** Time evolution of the energy, for the three different preparations described in the main text, compared with a quench from  $T = \infty$  to  $T = 1.4$  (top curve). In the three cases, the initial temperature is in the spin glass phase, and the final temperature is  $T = 1.4 > T_c$ . A very small ME is found at the time pointed by the arrow, only when warming up samples with similar starting energy.

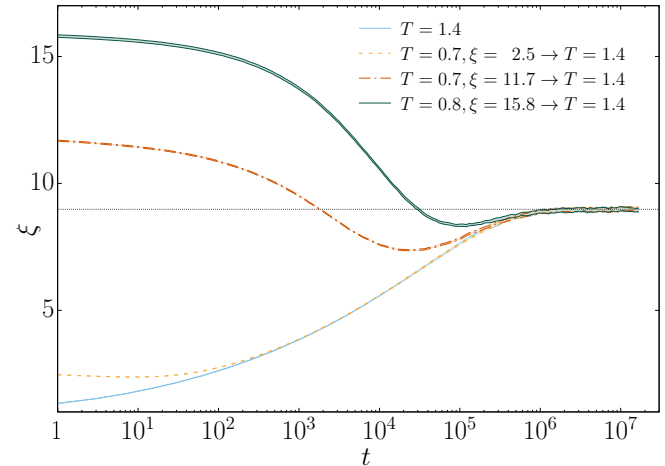


**Fig. 6. Coherence length: Undershooting and convergence to a master curve.** Coherence lengths  $\xi$  of the experiments described in Fig. 5. The time evolution of  $\xi$  tends to converge towards the curve corresponding to a quench from  $T = \infty$  to  $T = 1.4$  (bottom curve), giving rise to an undershoot of  $\xi$  when its initial value is higher than the equilibrium  $\xi$  at  $T = 1.4$ .

the approximate description afforded by Eq. (2) is accurate enough to explain the ME.

Our results explain how the most natural experimental setup (prepare two identical systems at  $T_1, T_2 > T_c$  with an identical protocol, then quench them) can fail to see the effect (6). Indeed, for spin glasses at least, a different starting  $\xi$  is required. Above  $T_c$ , where the growth rate of  $\xi$  does not depend on  $T$ , this means letting the hotter preparation evolve for longer time at the initial temperature before the quench. On the other hand, if we prepare the systems at  $T_1, T_2 < T_c$  and then bring them to an even lower temperature, the effect is enhanced, because in the  $T < T_c$  phase the growth of  $\xi$  is slower for lower temperatures. Therefore, in the low-temperature phase the ME can be found even with identical preparation times for the hot and cold preparations. Finally, we have investigated the Inverse ME (IME). If both the initial and

the final temperatures lie below  $T_c$  the system behaves in a symmetrical way under cooling or heating (see Fig. 4). On the other hand, if we start in the spin glass phase and end in the paramagnetic phase, the IME is strongly suppressed because Eq. (2) is not valid for  $T > T_c$ .

The ME is peculiar among the many memory effects present in spin glasses. Indeed, this phenomenon can be studied through quantities such as the energy density, which are measured at just one time scale (rather than the usual two times (17, 18, 23)). However, our setup poses an experimental challenge, because we are not aware of any measurement of the non-equilibrium temperature associated with the magnetic degrees of freedom. Perhaps one could adapt the strategy of Ref. (35), connecting dielectric susceptibility and polarization noise in glycerol, to measurements of high-frequency electrical noise in spin glasses (36).

An easier experimental avenue is suggested by our study of the inverse Mpemba effect, where the preparations are heated, rather than cooled. In this case, while the response of the energy is very small, the process is accompanied by a dramatic memory effect in the coherence length. This quantity has a non-monotonic time evolution upon heating from the spin-glass to the paramagnetic phase, before converging to the master (isothermal) curve and is measurable with current experimental techniques.

Our investigation of the Mpemba effect offers as well a new perspective into an important problem, namely the study of the glassy coherence length in supercooled liquids and other glass formers (37). Indeed, the identification of the right correlation function to study experimentally (or numerically) is still an open problem. Spin glasses are unique in the general context of the glass transition, in both senses: we know which correlation functions should be computed microscopically (38, 39), while accurate experimental determinations of the coherence length have been obtained (26). The fact that we have such a strong command over the spin-glass coherence length has allowed us to test to very high accuracy its relationship with an extremely simple quantity such as the energy, see Eq. (2). Furthermore, we have shown that this tight relationship between the coherence length and the energy holds only in the spin-glass phase. Yet, the energy is a local, single-time quantity just as the specific volume measured in the Kovacs effect in polymers. Therefore, Eq. (2) suggests an intriguing and far reaching alternative: rather than considering two-time correlation functions of ever-increasing complexity, it might be worth seeking high-accuracy experimental measurements of single-time quantities such as the specific volume. Furthermore, we find that the Mpemba effect is tiny, almost invisible, in the paramagnetic phase. Thus, finding a sizeable Mpemba-like behavior for quantities such as the specific volume may be a crucial step forward in the experimental identification of a glassy coherence length in a low-temperature phase.

## Materials and Methods

**Model and observables.** We consider Metropolis dynamics for the Edwards-Anderson model in a cubic lattice of linear size  $L = 160$ , with nearest-neighbor interactions and periodic boundary conditions:

$$\mathcal{H} = - \sum_{\langle \mathbf{x}, \mathbf{y} \rangle} J_{\mathbf{x}, \mathbf{y}} s_{\mathbf{x}} s_{\mathbf{y}}. \quad [3]$$

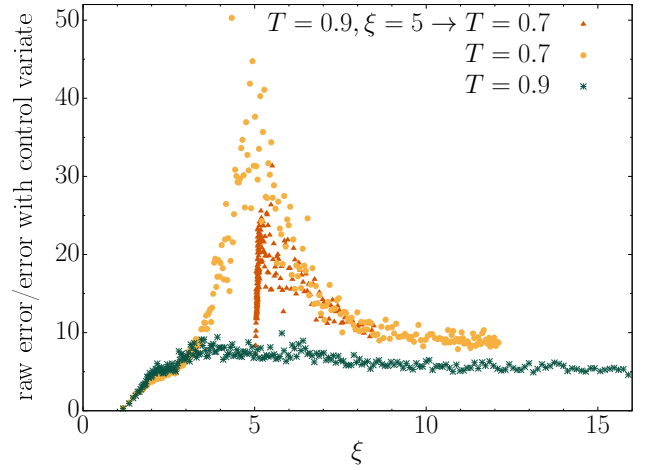


**Fig. 7. Improving the accuracy with control variates.** The figure shows the ratio of statistical errors, as a function of  $\xi(t)$ , for the naive [Eq. (6)] and improved [Eq. (8)] estimates of the energy density. The data shown correspond to three different relaxations. Two of them are isothermal relaxations starting from  $\xi = 0$  at  $t = 0$ . The third relaxation corresponds to the preparation starting at  $(T = 0.9, \xi = 5)$  which is quenched to  $T = 0.7$  at  $t = 0$  (i.e. the green curves in Figs. 3 and 4). The error reduction is largest for the isothermal relaxation at  $T = 0.7$  and  $2^{19} \leq t \leq 2^{21}$ , of course (after all, this is the temperature and time region defining the control variate), but the error reduction is also very significant at other times and temperatures.

The spins  $s_{\mathbf{x}} = \pm 1$  are placed on the lattice nodes,  $\mathbf{x}$ . The couplings  $J_{\mathbf{x}, \mathbf{y}} = \pm 1$ , which join nearest neighbors only, are chosen randomly with 50% probability and are quenched variables. For each choice of the couplings (one “sample”), we simulate 256 independent copies of the system (clones). We denote by  $\langle \dots \rangle_J$  the average over the thermal noise (i.e. average over results for the 256 clones corresponding to a single sample), the *subsequent* average over our 16 samples is indicated by square brackets  $[\dots]$ . The lattice size  $L = 160$  is large enough to effectively represent the thermodynamic limit (for this, and other details, see Ref. (25)). The model described by Eq. (3) undergoes a spin-glass transition at  $T_c = 1.102(3)$  (27). A single Metropolis sweep roughly corresponds to one picosecond of physical time. Therefore, the time in our simulations varies from one picosecond to a tenth of a second.

We compute the spin-glass coherence length from the decay of the microscopic correlation function

$$C_4(\mathbf{r}, t) = \frac{1}{L^3} \sum_{\mathbf{x}} [\langle q_{\mathbf{x}}^{(a,b)} q_{\mathbf{x}+\mathbf{r}}^{(a,b)} \rangle_J]. \quad [4]$$

where the overlap-field is computed as

$$q_{\mathbf{x}}^{(a,b)} = s_{\mathbf{x}}^{(a)} s_{\mathbf{x}}^{(b)}. \quad [5]$$

In the above expression, indices  $a$  and  $b$  label *different* clones (of course, we average over the  $256 \times 255/2$  possible choices for the pair of clones). Technically speaking, the spin-glass coherence length  $\xi$  employed in this work corresponds to the  $\xi_{1,2}$  integral determination (we refer the reader to the literature for details (24, 25)).

**The energy density and its control variate.** The naive determination of the internal energy density at time  $t$  ( $t$  is the time elapsed after the initial preparation, as measured in Metropolis full-lattice sweeps) is

$$E^{\text{naive}}(t) = \frac{1}{L^3} \overline{\langle \mathcal{H}(t) \rangle_J}. \quad [6]$$

This estimate, which is perfectly correct, can be made far more accurate by using a suitable control variate (30).

Before going on, it should be clear that  $E^{\text{naive}}(t)$  is a random variable: it is the estimate of the thermal and disorder average *as obtained from our numerical data*. Of course, the *exact* mean values, obtained by averaging over the thermal noise and the coupling realizations with infinite statistics, are not random variables.

Specifically, we improve  $E^{\text{naive}}(t)$  by subtracting from it another random variable, named the control variate, extremely correlated with it. The expectation value of the control variate vanishes, hence it does not change the (inaccessible with finite statistics) exact expectation value of  $E^{\text{naive}}(t)$ . Furthermore, we choose a control variate which is independent of temperature and time. So, the overall effect of the control variate is twofold: (i) a uniform (random) vertical shift for all data in Figs. 2–5 and (ii) a dramatic reduction of the error bars.

Our control variate is obtained as follows. For each of our 16 samples, we take a fully random initial configuration, place it suddenly at  $T = 0.7$  (this is our  $t = 0$ ), simulate it at constant temperature and, finally, compute

$$\mathcal{E}_J = \frac{1}{L^3 N_S} \sum_{t \in S} \langle \mathcal{H}(t) \rangle_J, \quad [7]$$

where  $S$  is the set of the  $N_S$  times of the form  $t = (\text{integer part of } 2^{n/8})$ , with  $n$  integer and  $2^{19} \leq t \leq 2^{21}$ . Besides, we obtain a high-accuracy estimate of the same quantity,  $\mathcal{E}^{\text{accurate}}$  by averaging over the results of a targeted simulation with 160000 samples and 2 clones (i.e. the energy is averaged over 320000 systems). The final estimates of the internal energy shown in Figs. 2–5 are

$$E(t) = E^{\text{naive}}(t) - [\mathcal{E}_J - \mathcal{E}^{\text{accurate}}]. \quad [8]$$

The benefits of using the control variate are obvious from Fig. 7.

**ACKNOWLEDGMENTS.** We strongly thank Raymond Orbach, Srikanth Sastry and Marija Vucelja for very interesting comments. This work was partially supported by Ministerio de Economía, Industria y Competitividad (MINECO), Spain, through Grants No. FIS2013-42840-P, No. MTM2014-56948-C2-2-P, No. FIS2015-65078-C2, No. FIS2016-76359-P, No. TEC2016-78358-R and No. MTM2017-84446-C2-2-R (Grants also partly funded by FEDER); by the Junta de Extremadura (Spain) through Grant Nos. GRU18079 and IB16013 (partially funded by FEDER) and by the DGA-FSE (Diputación General de Aragón – Fondo Social Europeo). This project has received funding from the European Research Council (ERC) under the European Union’s Horizon 2020 research and innovation program (Grant Nos. 694925 and 723955 - GlassUniversality). D.Y. acknowledges support by the Soft and Living Matter Program at Syracuse University. EM and DY thank the KITP and its “Memory Formation in Matter” programme, where contributions to the present work were developed, and acknowledge support from the National Science Foundation under Grant No. from NSF-PHY-1748958.

1. Mpemba EB, Osborne DG (1969) Cool? *Physics Education* 4(3):172–175.
2. Greaney PA, Lani G, Cicero G, Grossman JC (2011) Mpemba-like behavior in carbon nanotube resonators. *Metallurgical and Materials Transactions A* 42(13):3907–3912.
3. Ahn YH, Kang H, Koh DY, Lee H (2016) Experimental verifications of mpemba-like behaviors of clathrate hydrates. *Korean Journal of Chemical Engineering* 33(6):1903 – 1907.
4. Aristotle (1981) *Metaphysics (English translation by Ross, W.D.)*. (Clarendon, Oxford, UK).
5. Jeng M (2006) The mpemba effect: When can hot water freeze faster than cold? *American Journal of Physics* 74(6):514–522.
6. Burrige HC, Linden PF (2016) Questioning the mpemba effect: hot water does not cool more quickly than cold. *Scientific Reports* 6:37665.
7. Lu Z, Raz O (2017) Nonequilibrium thermodynamics of the markovian mpemba effect and its inverse. *Proceedings of the National Academy of Sciences* 114(20):5083–5088.

8. Lasanta A, Vega Reyes F, Prados A, Santos A (2017) When the hotter cools more quickly: Mpemba effect in granular fluids. *Phys. Rev. Lett.* 119(14):148001.
9. Klich I, Raz O, Hirschberg O, Vucelja, M. The mpemba index and anomalous relaxation. arXiv:1711.05829v3 (18 December 2018)
10. Kovacs AJ, Aklonis JJ, Hutchinson JM, Ramos AR (1979) Isobaric volume and enthalpy recovery of glasses. ii. a transparent multiparameter theory. *Journal of Polymer Science: Polymer Physics Edition* 17(7):1097–1162.
11. Lahini Y, Gottesman O, Amir A, Rubinstein SM (2017) Nonmonotonic aging and memory retention in disordered mechanical systems. *Phys. Rev. Lett.* 118(8):085501.
12. Struik CLE (1980) *Physical Aging in Amorphous Polymers and Other Materials*. (Elsevier, Amsterdam).
13. Fiocco D, Foffi G, Sastry S (2014) Encoding of memory in sheared amorphous solids. *Phys. Rev. Lett.* 112(2):025702.
14. Prados A, Trizac E (2014) Kovacs-like memory effect in driven granular gases. *Phys. Rev. Lett.* 112(19):198001.
15. Kürsten R, Sushkov V, Ihle T (2017) Giant kovacs-like memory effect for active particles. *Phys. Rev. Lett.* 119(18):188001.
16. Sasaki T, Ukyo Y, Novák P (2013) Memory effect in a lithium-ion battery. *Nature Materials* 12:569–575.
17. Jonason K, Vincent E, Hammann J, Bouchaud JP, Nordblad P (1998) Memory and chaos effects in spin glasses. *Phys. Rev. Lett.* 81(15):3243–3246.
18. Young AP (1998) *Spin Glasses and Random Fields*. (World Scientific, Singapore).
19. Baity-Jesi M, et al. (2014) Janus II: a new generation application-driven computer for spin-system simulations. *Comp. Phys. Comm* 185:550–559.
20. Marinari E, Parisi G, Ruiz-Lorenzo J, Ritort F (1996) Numerical evidence for spontaneously broken replica symmetry in 3d spin glasses. *Phys. Rev. Lett.* 76(5):843–846.
21. Berthier L, Bouchaud JP (2002) Geometrical aspects of aging and rejuvenation in the ising spin glass: A numerical study. *Phys. Rev. B* 66(5):054404.
22. Baity-Jesi M, et al. (2017) A statics-dynamics equivalence through the fluctuation–dissipation ratio provides a window into the spin-glass phase from nonequilibrium measurements. *Proceedings of the National Academy of Sciences* 114(8):1838–1843.
23. Baity-Jesi M, et al. (2017) Matching microscopic and macroscopic responses in glasses. *Phys. Rev. Lett.* 118(15):157202.
24. Belletti F, et al. (2009) An in-depth look at the microscopic dynamics of Ising spin glasses at fixed temperature. *J. Stat. Phys.* 135:1121.
25. Baity-Jesi M, et al. (2018) Aging rate of spin glasses from simulations matches experiments. *Phys. Rev. Lett.* 120(26):267203.
26. Guchhait S, Orbach RL (2017) Magnetic field dependence of spin glass free energy barriers. *Phys. Rev. Lett.* 118(15):157203.
27. Baity-Jesi M, et al. (2013) Critical parameters of the three-dimensional ising spin glass. *Phys. Rev. B* 88:224416.
28. Zhai Q, et al. (2017) Glassy dynamics in cumn thin-film multilayers. *Phys. Rev. B* 95(5):054304.
29. Fernández LA, Martín-Mayor V (2015) Testing statics-dynamics equivalence at the spin-glass transition in three dimensions. *Phys. Rev. B* 91(17):174202.
30. Fernandez LA, Martín-Mayor V (2009) Mean-value identities as an opportunity for Monte Carlo error reduction. *Phys. Rev. E* 79:051109.
31. Parisi G (1988) *Statistical Field Theory*. (Addison-Wesley).
32. Boettcher S (2005) Stiffness of the edwards-anderson model in all dimensions. *Phys. Rev. Lett.* 95(19):197205.
33. Fernández LA, Marinari E, Martín-Mayor V, Parisi G, Ruiz-Lorenzo J (2019) An experiment-oriented analysis of 2d spin-glass dynamics: a twelve time-decades scaling study. *J. Phys. A: Math. Theor.* 52:224002
34. Fernández LA, Marinari E, Martín-Mayor V, Parisi G, Ruiz-Lorenzo J (2018) Out-of-equilibrium 2d ising spin glass: almost, but not quite, a free-field theory. *Journal of Statistical Mechanics: Theory and Experiment* 2018(10):103301.
35. Grigera TS, Israeloff NE (1999) Observation of fluctuation-dissipation-theorem violations in a structural glass. *Phys. Rev. Lett.* 83(24):5038–5041.
36. Israeloff NE, Weissman MB, Nieuwenhuys GJ, Kosiorowska J (1989) Electrical noise from spin fluctuations in cumn. *Phys. Rev. Lett.* 63(7):794–797.
37. Cavagna A (2009) Supercooled liquids for pedestrians. *Physics Reports* 476(4):51–124.
38. Edwards SF, Anderson PW (1975) Theory of spin glasses. *Journal of Physics F: Metal Physics* 5:965.
39. Edwards SF, Anderson PW (1976) Theory of spin glasses. ii. *J. Phys. F* 6(10):1927.